2016-08

Development of a user experience enhanced teleoperation approach

Chen, J

http://hdl.handle.net/10026.1/15866

Development of a User Experience Enhanced Teleoperation Approach

Junshen Chen, Marc Glover, Chunxu Li and Chenguang Yang*

Abstract— In this paper, we have investigated various techniques that can be used to enhance user experience for robot teleoperation. In our teleoperation system design, the human operator are provided with both immersive visual feedback and intuitive skill transfer interface such that when controlling a telerobot arm, a user is able to "feel" in a first person perspective in terms of both visual and haptic sense. A number of high-tech devices including Omni haptic joystick, MYO armband, Oculus Rift DK2 headset, and Kinect v2 camera are integrated. The surface electromyography (sEMG) signal allows operator to naturally and efficiently transfer his/her motion skill to the robot, based on the properly designed elastic force feedback. For visual feedback, operators can control the pose of a camera on the head of the robot via the wearable visual headset, such that the operator is able to perceive from the robot's perspective. Extensive tests have been performed with human subjects to evaluate the design, and the experimental results have shown that superior performance and better user experience have been achieved by the proposed method in comparison with the traditional methods.

I. Introduction

Unmanned robots which complete tasks autonomously have been popular in industrial applications, as these robots can complete tasks which require high precision, minimal completion time, and even in the extreme environments that are hazardous to our humans. However, specialised tasks involving uncertain issues, e.g., medical operation, are not suitable for a fully-autonomous robots to complete. It is desired that a human operator tele-control a robot for these tasks according to [1], i.e., teleoperation.

For teleoperation, haptic and visual information for coordinated feedback play significant roles that affect the user experience. Immersive visual feedback technique has been utilised in many research projects to provide an operator with a sense of telepresence [2] [3], i.e., the feeling that the operator exists at the robot's remote location. An Oculus Rift headset is used in this work to give an immersive visual feedback of the workspace of a robotic arm, from a fixed position stereo camera in [4]. However, this system does not allow an operator to manipulate the orientation of the stereo camera. An underwater simulation environment is created in [5], and it allows an operator to control the orientation and operators view of a simulated ROV (Remotely

Operated Vehicle), via an Oculus Rift headset. In comparison to this design, our design is based on a physical platform. By combining haptic feedback, and visual feedback, an operator would naturally experience telexistence [2]. However, none of the research mentioned above investigate whether there is a link between operator task performance and operator immersion whilst teleoperating (telexistence). Therefore, extensive tests have been performed in this work to compare the effects of immersive and non-immersive teleoperation interfaces on operator task performance.

Haptic feedback devices are also commonly used in teleoperation. They have been implemented by numerous researchers to give an operator force feedback from a telerobot [6] [7]. Most of these systems use force sensors at the end effector of the robotic arm [6], or calculate the force feedback via end effector collisions virtually [7], or physically through custom joint force sensors [8]. In this paper, we want the haptic feedback device can help to transfer human skills to the telebot.

To help transferring human mechanical motion and skills to robot, various kinds of technologies are applied by using different mathematical models and sensors. sEMG signal is one of these approaches and it is an ideal bio-signal to incorporate human skills into robots. sEMG is a relatively cheap and totally non-invasive technique to measure human muscular activity[9]. It can represent human joint torque [10], muscular force [11], finger motion [12], etc.. Moreover, with its easy accessibility and extensive adaptability, sEMG were widely used to cooperate with other sensors in many applications [13]. sEMG is a functional tool for letting robot understand human motions.

To gain better user experience while teleoperation, this paper introduced an immersive teleoperation system consist of a 3D stereo vision head set combined with tactile feedback force (proximity force). sEMG signals are collect while applying another tactile feedback force, elastic force. This tactile feedback force can result a remarkable result on skills transfer between human and robot and help the operator teleoperate the robot more intuitively.

II. Setup of Teleoperation using Baxter Robot

To enhance the telepresence, in this work, Oculus Rift DK2 that could provide vision from robot's perspective is employed (Fig. 1), together with haptic device Omni (Fig. 1), to teleoperate a Baxter robot arm (Fig. 1). This haptic device is of 6 degree-of-freedom (DOF), in which allows the user to preceive the obstacle and environment related forces. The forward kinematics, inverse kinematics and Jacobian

of the Omni haptic device has been well studied by [14]. In addition, infrared (IR) sensor's built into the cuff of Baxter's end-effector, are used to provide haptic feedback information to an operator about the distance between the robot's gripper and an object/surface (referred to as *proximity force*). The whole haptic feedback, is combined with two force feedbacks: referred to as *proximity force* (Fig. 4), and *elastic force* (Fig. 6), respectively, to provide a compound haptic feedback to the operator. And then, by wearing Myo armband (Fig. 1), the sEMG signal was collected from the operator and used to transfer skills from human operator to the robot.
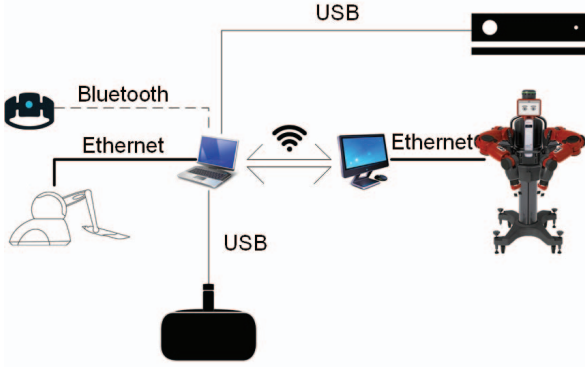

Fig. 1: The illustration of the teleoperation system.

A. Robot System Dynamics

In this paper, we implement multiple-input-multiple-output (MIMO) dynamics on a 7 DOF robot manipulator, Baxter robot, which we used for our previous work [15]. The dynamics equation of the robot manipulator can be described as the follows [16]:

$$M(q)\ddot{q} + C(q,\dot{q})\dot{q} + G(q) = \tau \tag{1}$$

where $M(q) \in R^{n \times n}$ is the manipulator inertia matrix, $C(q) \in R^{n \times n}$ is the Coriolis matrix for the manipulator, and τ denotes the control input.

The torque control input is designed as below, and it depends on a gain which will be decided by the operator's muscle activities reflected by the sEMG signals (see Section. IV-B):

$$\tau = \kappa \left(J_b^{-1} k_e (x^* - x) - \dot{\theta} \right) \tag{2}$$

where κ is the control gain which calculated by processing the sEMG signals, to be defined in Section. IV-B (11), J_b is the Jacobian matrix of the Baxter robot manipulator, k_e is a designed ratio for position error, x is the robot's trajectory, x^* is the reference trajectory commanded by the operator, which is obtained by applying transformation on $x^{*\prime}$, referring to our previous work [17] (as shown in Fig. 2), and $\dot{\theta}$ is the joint velocities of the manipulator.
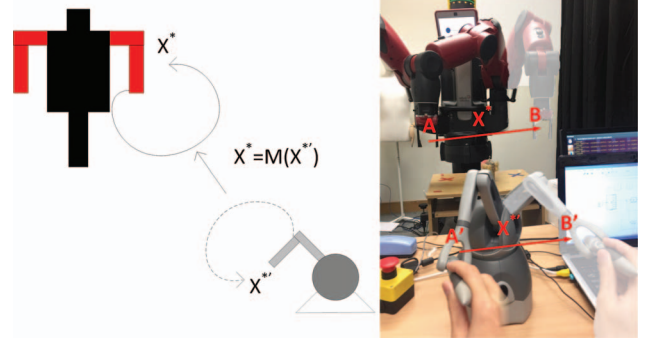

Fig. 2: Trajectory and reference trajectory generated by the Omni and the Baxter.

B. Oculus Rift

Oculus Rift is a head-mounted display, which uses the position tracking sensor and optical lens to consist a system, that the wearers can feel an illusion that they are actually in a virtual environment. In particular, Development Kit 2 (DK2) is used in this paper, which has developed four key improvements compare with DK1. The DK2 has higher resolution (960×1080 per eye), low-persistence OLED display, higher refresh rate, and positional tracking function.

(a) Oculus Rift DK2   (b) Myo Armband

Fig. 3: Oculus Rift DK2 and Myo armband.

C. MYO Armband

MYO armband, developed by the Thalmic Labs company, is a wearable device, which can recognise the hand gesture and arm movement, by wearing it on the arm. Based on the muscles movement, the 8 built-in EMG sensors, along with a 9-axis IMU sensor are able to identify the hand gesture and send the signals to system via Bluetooth. The sensors generate data by electrical impulses from arm muscles, and each user has different type of skin, muscle size and etc. It is necessary to calibrate the device before each different user start using. It can help to increase the accuracy of the gesture recognising performance.

III. IMMERSIVE VISUAL FEEDBACK

In this section, the proximity force and the 3D stereo vision are introduced. As by combining these two tactile and vision feedback, the system can provide the user a more immersive teleoperation experience.

A. Proximity Force

In order for the operator to sense that an object is close to the gripper, it is required that the pitch and yaw of the end effector, are known. By adding an extra point (P_W in Cartesian space) to the wrist of Baxter's right arm, it is possible to determine the direction that the end effector is pointing to in Cartesian space, represented as a resultant vector in Eq. 3:

$$P_s \overset{\text{def}}{=} \begin{bmatrix} x & y & z \end{bmatrix}^T ; P_{offset} \overset{\text{def}}{=} P_W - P_E \qquad (3)$$

where P_s is any Cartesian point in Baxter's workspace, including x, y, z coordinates, P_W is the added wrist point, P_E is the end effector point, and $P_{offset} \in R^3$ is the resultant vector. The magnitude of the resulting vector, is determined by the output value of the IR sensor on the end effector of the Baxter robot. The range of distances detectable by the end effector IR sensor is 40mm (closest) to 400mm (furthest), therefore, before this value (scalar) can be multiplied by the end effector direction vector, the detected distance must be subtracted from the maximum detectable distance, since the closer the object, the greater the magnitude of the force feedback the operator should experiences, and conversely the further away the object/surface, the smaller the magnitude of the force feedback the operator experiences. The resulting Cartesian force vector is analogous to a spring, between the end effector IR sensor, and the object detected (as shown in figure 4). The resulting Cartesian force vector is determined by Eq. 4:

$$F_p = P_{offset} \cdot k \left(d_{IRmax} - d_{object} \right) \qquad (4)$$

where $F_p = \begin{bmatrix} F_{px} & F_{py} & F_{zp} \end{bmatrix}^T$, k is a distance gain, $d_{IRmax} = 400mm$, and d_{object} is the IR sensed distance to the object.
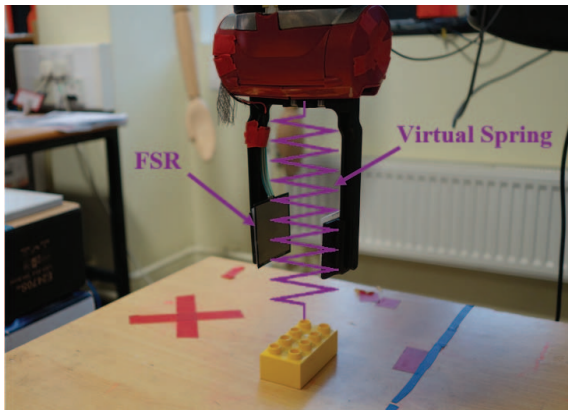

Fig. 4: Depicts the spring-like behaviour of the object proximity force feedback (derived from end effector IR sensor measurements, equation 4); an Interlink Electronics 406 force sensing resistor is attached to the left gripper pincer.

B. Visual feedback from the robot's perspective

A Kinect v2 device is mounted onto the head of Baxter to give the operator a complete view of the robot's workspace and a 3D printed mount was designed to fit directly onto the head of Baxter, as shown in Fig. 5(a). The Kinect v2 is mounted upon a 3D printed support bar, which fixes to an aluminium bracket. The aluminium bracket is fixed to a Dynamixel MX28R servo (tilt servo), which mounts on top of a Dynamixel MX28R servo (pan servo).

Controlling Kinect's View: The positions of both pan and tilt MX-28R servos are controlled by an Arduino Microcontroller Development board. The operator can view the entirety of Baxters workspace through the Oculus rift (via the Kinect v2) by changing the orientation of their head (Fig. 5). This gives the operator the ability to control the direction of the Kinect device from their head position.

(a)   (b)

Fig. 5: (a) The movement of the Kinect camera, determined by the head movements of operator. (b) The natural head movements of the operator, tracked by the headsets built-in IMU.

Rendering on Oculus Rift: To display images on the screen of the Oculus Rift headset: a program is used to implement D3D11 to create a 2D texture from the supplied colour image (Kinect or end effector camera), then present this to the Oculus, which will apply distortion, and scaling to the supplied texture, as well as reducing motion blur. Applying a distortion to original image cancels distortion contributed by the Oculus Rift's lenses. The final image is presented to each of the operator's eyes via the headset's screen. The 1920 x 1080 pixel screen is split into two halves (each 960 x 1080 pixels), both halves are presented with the same image in this system.

IV. INTUITIVE SKILL TRANSFER

In this section, the elastic force feedback and the extraction of muscle activation are introduced. By applying elastic force feedback on the haptic device, the operator will naturally generate force while tele-operating in order to counter the feedback force. So that the user can transfer his/her skills more intuitively to the robot while teleoperation.

A. Elastic Force Feedback

Rather than the traditional way of measuring interaction force, by mounting a force sensor onto the robot manipulator, we produce force feedback by a haptic rendering algorithm. The algorithm is obtained by the tracking error during
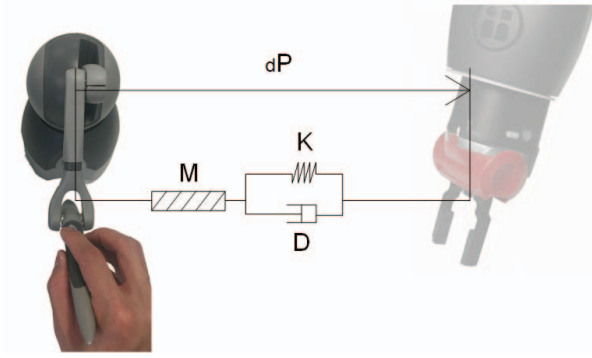
Fig. 6: Force feedback generation.

Fig. 7: Human Arm stiffness Mapping to Robot Joint.

motion. In Fig. 6, there is the admittance model we developed which helps to generate the elastic force feedback, and it's followed by the specified law below:

$$F_e = Md\ddot{P} + Dd\dot{P} + KdP \qquad (5)$$

where K is a virtual spring's stiffness, D is a virtual damper's damping ratio, M is an virtual mass and dP is the position difference between the Omni joystick's commanded reference position and the Baxter end-effector's actual position. In this paper, we only consider the 3 dimension translational motion for easy calculation, and $dP = P_s - P_m$, where $P_s \in R^3$ is the actual translational position of the Baxter's end-effector and $P_m \in R^3$ is the Omni device's reference position. So that, we can give the torque of the Omni as below:

$$\tau_o = J_o^{\mathrm{T}}(F_e + F_a) \qquad (6)$$

where τ_o is the torque of the Omni device, and J_o is the Jacobian matrix of the Omni device.

$$F_a = J^T \cdot \begin{bmatrix} F_{py} & F_{pz} & F_{px} \end{bmatrix}^T \qquad (7)$$

where the force vector is rearranged to match the Baxter and Omni's coordinate frames, $T = \begin{bmatrix} T_{J1} & T_{J2} & T_{J3} \end{bmatrix}^T$, and $J \in R^{3 \times 3}$ is the Jacobian matrix.

The elastic force generated by the haptic rendering algorithm (5) can help human operator to improve awareness of the tracking performance, i.e., combine visual sensing into the tactile sensing. Above all, the human operators will subconsciously grow force on their arm in order to counter the increased feedback force on the haptic device. That is because the feedback force will tend to pull/push the user's hand due to the difference between actual moving direction and the lagged robot end-effector position or overshoot position. So that the control gain will increase or decrease respectively according to the sEMG signals, and the robot manipulator will increase speed or slow down to match the user's action.

B. Extraction of Muscle Activation

The estimation of muscle activation level from raw sEMG signals will impact the performance of the human-robot skill transfer. So that the transformation of raw sEMG data to muscle activation level is an essential step for the experiment.
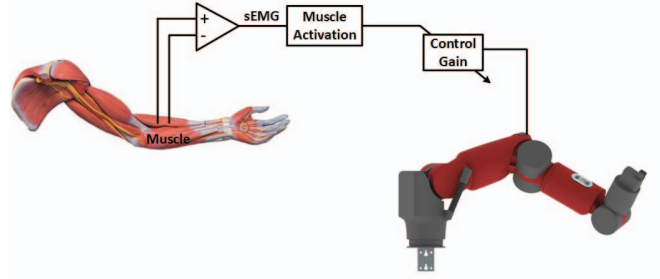
At first, all the 8 channels of raw sEMG signals obtained from the Myo armband, will be squared and low-pass filtered (see Fig. 8), according to our previous work [18].

Then recursive filter is appiled to determine the neural activation $u(t)$, by a rectified, normalised and filtered sEMG input $e(t)$. sEMG was represented below showing its time-varying feature [19]:

$$u(t) = \alpha * e(t-d) - \beta_1 * u(t-1) - \beta_2 * u(t-2) \qquad (8)$$

where d is the electromechanical delay, and α, β_1, β_2 are second-order dynamics' coefficients. In order to make sure (8) always have a positive stable solution, we must have:

$$\beta_1 = \gamma_1 + \gamma_2 \quad \beta_2 = \gamma_1 * \gamma_2 \quad \alpha - \beta_1 - \beta_2 = 1 \qquad (9)$$

where $|\gamma_1| < 1$, and $|\gamma_2| < 1$.

Then, as we explained in our previous paper [20], there is a nonlinear relationship between frequency and force for single motor units. And here is the nonlinear mapping method from $u(t)$ to muscle activation $a(t)$ [19]:

$$a(t) = \frac{e^{Au(t)} - 1}{e^A - 1} \qquad (10)$$

where $A \in [-3, 0]$ is the nonlinear shape factor. It can affect muscle activation level from $A = -3$ being highly exponential to $A = 0$ being linear.

In addition, if the control gain is setting proportionally to the muscle activation level, control rate and stiffness variations could result instability and incompatibility of the system. So that we normalise the control gain κ at the tth sampling instant within specified range as:

$$\kappa(t) = (\kappa^{max} - \kappa^{min}) \frac{(a(t) - a^{min})}{(a^{max} - a^{min})} + \kappa^{min} \qquad (11)$$

where κ^{max} and κ^{min} are the stable robot motion's gain range, a^{max} and a^{min} are the maximum and minimum muscle activation. These parameters can all be obtained experimentally beforehand.

V. EVALUATION OF SYSTEM PERFORMANCE

A. Test of Visual Immersion

Twelve subjects participated in testing, where they were asked to complete a simple pick up and place task, which
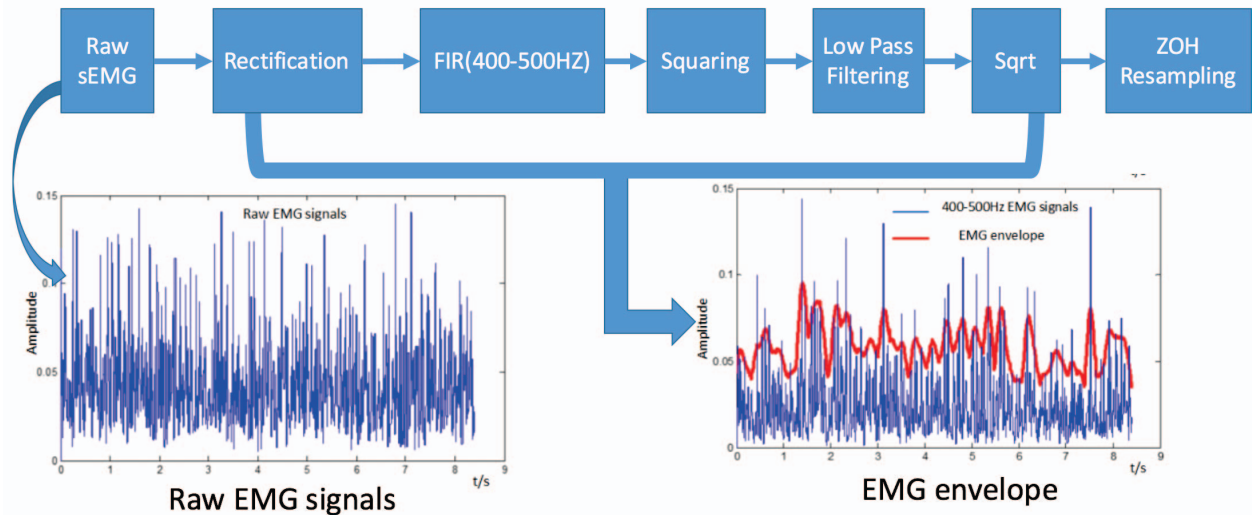
Fig. 8: sEMG signals processing procedure by using Squaring and Low-pass Filter.

involved stacking 3 Lego blocks on top of one another and picking up one block at a time, as shown in Fig. 9. This task was repeated for three different variations of the teleoperation system: the first system, the operator controlled the Kinect's position with the headset, was given force feedback when controlling the position of Baxter's right end-effector, and could switch between the Kinect and cuff camera's view. The second system, the operator was not presented with any force feedback when controlling the position of Baxter's right end effector. The third system, the operator did not wear the Oculus visual headset, instead the Kinect images were presented to the operator via an LCD monitor. The testing environment is shown in Fig. 9.

Operators were asked to complete a testing questionnaire after completing the task for each of the system variations, which asked the operator to rate various aspects of the each system. Whilst the operator was completing each task, the number of times that any part of the end effector collided with either the testing table or Lego blocks, as shown in Fig.10(a).
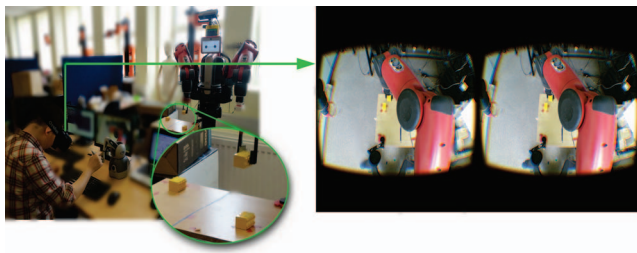

Fig. 9: An operator attempts the pick and place task using the Oculus Rift, and haptic controller (force feedback enabled)

According to the test results, 67% of the participant operators preferred the use of the Oculus Rift to supply visual feedback, instead of an LCD monitor. The remaining 33% preferred the LCD monitor, due to discomfort when viewing

images through the Oculus Rift headset.

Several operators expressed that they experienced difficulties when determining distance of objects from Baxter's right end effector when viewing Baxter's workspace via the Kinect. Coincidentally, 92% of operators said they prefer utilising the combination of Kinect and cuff camera views to pick up and place objects when completing the given tasks, rather than solely viewing images from the Kinect.
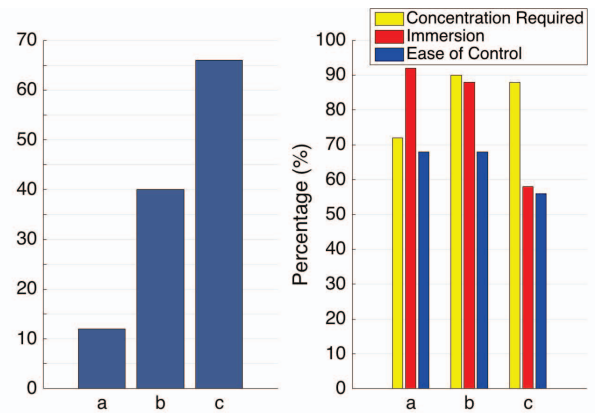

Fig. 10: (a) Correlation between interface type and total number of end effector table collisions; based on all 12 participants. aa. Visualization in robot's perspective + Haptic feedback. ab. Visualization in robot's perspective Only. ac. Screen + Feedback. (b) Average experience ratings of each system variant, reported by all participating operators. ba. Visualization in robot's perspective + Haptic feedback. bb. Visualization in robot's perspective Only. bc. Screen + Feedback.

Comparing Figs. 10(a) and 10(b), a relationship becomes apparent between the number of end effector collisions, and the level of immersion experienced by the operator. As the operators sense of immersion decreases, the number of end effector table collisions increases. The lack of depth sense

when viewing the robot workspace via the LCD screen or third-person visual headset, causes the operator to collide with the test table. Additionally, the lack of sense of depth the operator experiences via visual feedback, can also be improved by end effector-object proximity haptic feedback.

After comparing third-person visualisation & haptic feedback with screen & feedback (Fig. 10(b)), it can be seen that the immersiveness of the operator's experience can affect the concentration required for the operator to complete the given task. Average operator third-person visual experience is at 93% when using the Oculus Rift headset and 57% when presenting Baxter workspace images via the LCD screen relate to average operator, required concentration ratings of 73%, and 88% respectively. The increase in concentration required for the third-person visualisation only system compared to the third-person visualisation & haptic feedback system (Fig. 10(b)), can be attributed to the lack of force feedback in the third-person visualisation only system. 92% of tested operator's agreed that the haptic controller force feedback was helpful when moving the controller joints back to their respective initial positions, after the operator has switched from the cuff camera to the Kinect camera view, or the operator has finished changing the position of the right end effector gripper pincers. However, 58% of those who agreed, commented that the force feedback was too strong and uncomfortable at times, i.e. the force feedback would sometimes spike, giving the operator a large force for a small period of time (approximately 0.1 seconds).
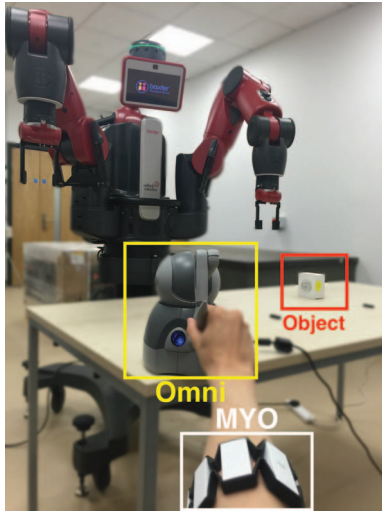
B. Intuitive Skill Transfer

Fig. 11: Designed Pick-up and Place task setup.

In this set of the experiments, the manipulator's tracking speed can be adjusted online. A pick-up and place task is designed to verify whether the sEMG based teleoperation can help user to have a more intuitive teleoperation experience, and can improve the tracking performance in terms of
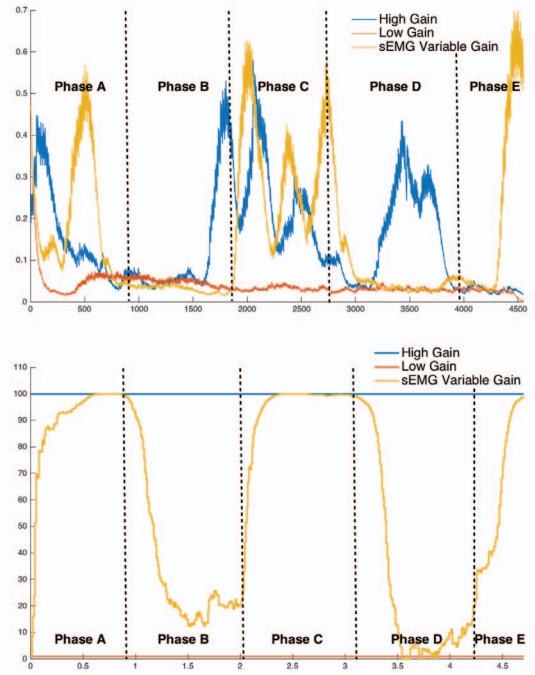

Fig. 12: a. End-effector Speed of Baxter robot. b. Control gain value of Baxter robot. Phase A: Approaching the object. Phase B: Picking up the object. Phase C: Moving to the placing area. Phase D: Placing the object. Phase E: Moving back to the initial position.
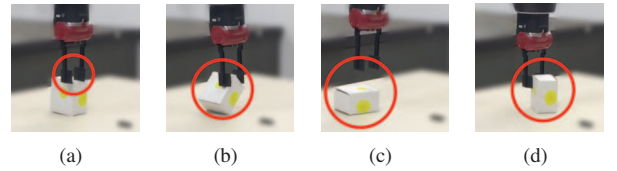

Fig. 13: Set of screen shots of the recorded test tries under high gain control mode.

efficiency and accuracy. In the experiments, the global task objective is to pick up the target object from a start position, and then place it to a target position, as shown in Fig. 11. Different types of control gains will be applied on each task.

The control gain was set to high, low and variable as extracted from user's sEMG in different iteration of the experiment for comparative studies. In Fig. 12, the blue line represents the tracking speed when the control gain was set to high. The tracking performance was good due to its high following speed. However, it is difficult to perform high accuracy required movement such as pick-up the target object. As we can tell from a set of screen shots of the recorded test tries (Fig. 13), the manipulator will either miss the object or knock over/move the object from its original position.

The yellow line in Fig. 12 represents the tracking speed when the control gain is sEMG variable based. In Phase A,

when we need to fast approach the object, the control gain immediately increased and almost reach the same level as in the high gain mode. Then it dropped to a controllable level when need to pick up the object, in Phase B. It raised back to a high level after the object was picked up and remain the level until the operator made the robot arm move to the placing area, as shown in Phase C. Then the control gain immediately dropped again when the operator did the place manoeuvre, as in Phase D. Finally, the control gain raised back when the operator moved the manipulator to its initial position, as in Phase E.

The red line in Fig. 12 shows the tracking speed when the control gain was set to low. The manipulator was able to finish the task and the performance was accurate due to its relatively slow speed. However, it is time consuming for finishing the same task compare with the previous two control gain set. The time consumption of finishing the entire task in the sEMG based variable gain mode almost matches that in the high gain mode, while it is two times longer of that in the low gain mode.

With these comparative experiments, the sEMG variable gain control mode ensures a more accurate, smooth and efficient teleoperation experience than the other two modes. Furthermore, it is more intuitive for the untrained, unskilful operators to transfer their skills to robot.

VI. Conclusion

In conclusion, visual feedback from the robot's perspective is provided combined with compound haptic feedback for teleoperating a robot arm. sEMG signals are collected to vary the control gain of the manipulator. Using Oculus Rift headset, the visual feedback provided enables an operator to view robot workspace in the robot's perspective. This greatly assists the operator in concentrating on completing the task, whilst reducing the cognitive load on the user, since the operator is able to move their head in a natural way to manipulate the position of the camera on robot's head. Wearing Myo armband, the sEMG signal enables the operator to teleoperate the robot more intuitively, since the control gain will be changed while the user naturally countering the force feedback generated on the haptic device. Experimental test results show that most tested operators preferred using the Oculus Rift headset for visual feedback of the robot workspace, and the tracking performance become better when sEMG applied. The visual and haptic feedback techniques investigated in this work help to improve user experience in both immersive and intuitive ways, and can be applied in similar teleoperation setup.

References

[1] A. Sarmah and U. Gulhane, "Surgical robot teleoperated laparoscopic grasper with haptics feedback system," in *Emerging Trends in Robotics and Communication Technologies (INTERACT), 2010 International Conference on*, Dec 2010, pp. 288–291.

[2] S. Tachi, K. Komoriya, K. Sawada, T. Nishiyama, T. Itoko, M. Kobayashi, and K. Inoue, "Telexistence cockpit for humanoid robot control," *Advanced Robotics*, vol. 17, no. 3, pp. 199–217, 2003. [Online]. Available: http://dx.doi.org/10.1163/156855303764018468

[3] V. Do, I. Longshore, D. Mally, and S. Raper, "Lakitu: Long-range aerial kinetic immersive telepresence unit," 2015, available: http://robohub.org/wp-content/uploads/2013/04/BaxterResearch.jpg. Accessed: 2015-08-20. [Online]. Available: http://www.seas.upenn.edu/~cse400/CSE400_2014_2015/reports/05_report.pdf

[4] D. Pamungkas and K. Ward, "Immersive teleoperation of a robot arm using electro-tactile feedback," in *Automation, Robotics and Applications (ICARA), 2015 6th International Conference on*, Feb 2015, pp. 300–305.

[5] C. Ha, S. Park, J. Her, I. Jang, Y. Lee, G. R. Cho, H. I. Son, and D. Lee, "Whole-body multi-modal semi-autonomous teleoperation of mobile manipulator systems," in *Robotics and Automation (ICRA), 2015 IEEE International Conference on*, May 2015, pp. 164–170.

[6] T. Horie, N. Abe, K. Tanaka, and H. Taki, "Controlling two remote robot arms with direct instruction using hapticmaster and vision system," *ICAT2000*, pp. 167 – 172, 2000.

[7] A. Leeper, S. Chan, K. Hsiao, M. Ciocarlie, and K. Salisbury, "Constraint-based haptic rendering of point data for teleoperated robot grasping," in *Haptics Symposium (HAPTICS), 2012 IEEE*, March 2012, pp. 377–383.

[8] A. Marchese and H. Hoyt, "Force sensing and haptic feedback for robotic telesurgery," Master's thesis, Worcester Polytechnic Institute, 2010.

[9] J. Vogel, C. Castellini, and P. van der Smagt, "Emg-based teleoperation and manipulation with the dlr lwr-iii," in *Intelligent Robots and Systems (IROS), 2011 IEEE/RSJ International Conference on*, Sept 2011, pp. 672–678.

[10] R. Osu, D. W. Franklin, D. W. Franklin, H. Kato, H. Kato, H. Gomi, H. Gomi, K. Domen, K. Domen, T. Yoshioka, T. Yoshioka, M. Kawato, and M. Kawato, "Short- and long-term changes in joint co-contraction associated with motor learning as revealed from surface emg," *J Neurophysiol*, vol. 88, p. 2002, 2001.

[11] G. C. Ray and S. K. Guha, "Relationship between the surface e.m.g. and muscular force," *Medical and Biological Engineering and Computing*, vol. 21, no. 5, pp. 579–586. [Online]. Available: http://dx.doi.org/10.1007/BF02442383

[12] K.-J. You, K.-W. Rhee, and H.-C. Shin, "Finger motion decoding using emg signals corresponding various arm postures," *Experimental neurobiology*, vol. 19, no. 1, pp. 54–61, 2010.

[13] N. Wang, C. Yang, M. R. Lyu, and Z. Li, "An emg enhanced impedance and force control framework for telerobot operation in space," in *2014 IEEE Aerospace Conference*, March 2014, pp. 1–10.

[14] T. Sansanayuth, I. Nilkhamhang, and K. Tungpimolrat, "Teleoperation with inverse dynamics control for phantom omni haptic device," in *SICE Annual Conference (SICE), 2012 Proceedings of*. IEEE, 2012, pp. 2121–2126.

[15] C. Yang, J. Chen, Z. Li, W. He, and C. Y. Su, "Development of a physiological signals enhanced teleoperation strategy," in *Information and Automation, 2015 IEEE International Conference on*, Aug 2015, pp. 13–19.

[16] F. H. Ghorbel, O. Chetelat, R. Gunawardana, and R. Longchamp, "Modeling and set point control of closed-chain mechanisms: theory and experiment," *IEEE Transactions on Control Systems Technology*, vol. 8, no. 5, pp. 801–815, Sep 2000.

[17] Z. Ju, C. Yang, Z. Li, L. Cheng, and H. Ma, "Teleoperation of humanoid baxter robot using haptic feedback," in *Multisensor Fusion and Information Integration for Intelligent Systems (MFI), 2014 International Conference on*, Sept 2014, pp. 1–6.

[18] P. Liang, C. Yang, Z. Li, and R. Li, "Writing skills transfer from human to robot using stiffness extracted from semg," in *Cyber Technology in Automation, Control, and Intelligent Systems (CYBER), 2015 IEEE International Conference on*, June 2015, pp. 19–24.

[19] Z. Xiao, Z. Li, and M. Chen, "Position/force estimation using hill muscle model incorporating adaboost with svm-based component classifiers," in *Intelligent Control and Automation (WCICA), 2014 11th World Congress on*, June 2014, pp. 1923–1928.

[20] C. Yang, J. Chen, Z. Li, W. He, and C.-Y. Su, "Development of a physiological signals enhanced teleoperation strategy," in *Information and Automation, 2015 IEEE International Conference on*. IEEE, 2015, pp. 13–19.